Aerial images and LIDAR Fusion Applied in Forest Boundary Detection

Zuyuan Wang, Ruedi Boesch, Christian Ginzler
Dept. of Land Resource Assessment, Swiss Federal Research Institute WSL,
Zuercherstr. 111, CH-8903 Birmensdorf
SWITZERLAND

Abstract: -Forest boundary delineation is one of the key issues of forest management for Swiss National Forest Inventory (NFI). The proposed approach in this paper focuses on the detection of forest boundaries with special emphasis on spatially contiguous and reproducible results by using both aerial images and LIDAR data. The used Green Vegetation Index (GVI) is helpful to find green vegetation areas while the curvature feature curvature features extracted from the canopy height model (CHM) is helpful for building removing, The combination of curvature features, GVI, JSEG segmentation result and the Gabor wavelet texture features leads to forest area detection and obtains proper forest boundaries. Preliminary results are encouraging, regarding an automatic process and delivers robust forest boundary detection.

Key-Words: Aerial images, Image segmentation, LIDAR, Gabor wavelet, Forest Inventory, Texture features

1 Introduction

Switzerland ranks second with Germany as the most densely forested country in Europe, with 30% of its territory covered by forest. As we know, forest plays an essential part in preserving the landscape and performs various tasks. For example, it helps to prevent landslides and erosion, reduce flooding and prevent avalanches. It provides wood production, non-wood production like game, honey and mushrooms. It acts as a windbreak and helps to purify the air. In 1981, the Swiss Federal Council decided to carry out the first National Forest Inventory (NFI)[1-3] to record the current state and the changes of the Swiss forest in all its functions for management. With the ongoing third NFI (NFI3), there are about 7000 aerial images covering the whole of Switzerland which can be used for extracting forest features.

Forest boundary is one of the important forest parameters for forest managements. In NFI, forest boundaries are interpreted at each sample plot belonging to a regular 500m grid with 25 raster points. Height and surface cover information is gained by interpreters and then a forest boundary line is measured. However, with such kind of coarse grid sampling design in NFI, it is not suitable for local assessment of forest stands. Hence spatially contiguous and automatic boundary detection of forest-stands is one of the prerequisites to overcome such limitations.

LIDAR (LIght Detection and Ranging data) is a term used for a method of distance measurement using laser light. With its application used in aerial laser scanning**,** it provides rich information on the vertical structure of forest.[4] A number of studies reveal the successfully use of LIDAR -based techniques to estimate tree and stand attributes such as height, crown diameter, basal area and stem volume.[5, 6]

In recent years, technological improvements of remote sensing in data acquisition and processing have provided better decision tools for forest planning management activities.[7] For example, multi-spectral imagery as both obtained by airborne and spaceborne sensors can be useful in forest management for determining forest stand boundaries, species composition, feature locations and the detection of dead trees. Furthermore, high resolution aerial images improve efficient forest management at fine scale.[8, 9] The need for the use of image segmentation in remote sensing -based forestry applications were recognized during the 1980s, when the studies began concerning the applicability of Landsat TM and SPOT images to forest inventories.[10] Direct forest stand delineation can be found such as by image segmentation of satellite data.[11] However, A VHR (Very High Resolution) image of a forested area is a composition of certain spectral classes, such as shaded crown, and ground pixels. The spectral properties of the neighboring pixels within a stand may be very different. Therefore simple segmentation will lead to unsatisfactory results due to the high local variation.

This paper makes it is possible to merge features from both LIDAR data and aerial images to propose a semantics segmentation of forest area in a meaningful way. Empirical tests show that the proposed method offers an automatic process of forest boundary detection for various aerial images in a promising way.

2 Material and Methods

2.1 Method overview

Fig. 1 illustrates a schematic workflow of the proposed forest boundary detection method. Aerial imagery and LIDAR data are data sources used in the method. From the given LIDAR point clouds, DTM and DSM are obtained. Based on DTM and DSM data, a CHM (Canopy Height Model)-grid has been used in our study. Furthermore, curvature features of the CHM are calculated for the purpose of removing building areas. Meanwhile, a green vegetation index (GVI) is gotten based on the ratio of green band and red band in RGB color space of aerial images for the aim of achieving forest area candidates. Each aerial image is segmented by using JSEG segmentation to get initial homogeneous sub areas. Combining with CHM, curvature features and GVI, some real forest areas can be obtained from the initial JSEG segmentation results. At last, Gabor wavelet texture features are used in order to detect all forest areas so that forest boundary can be delineated.

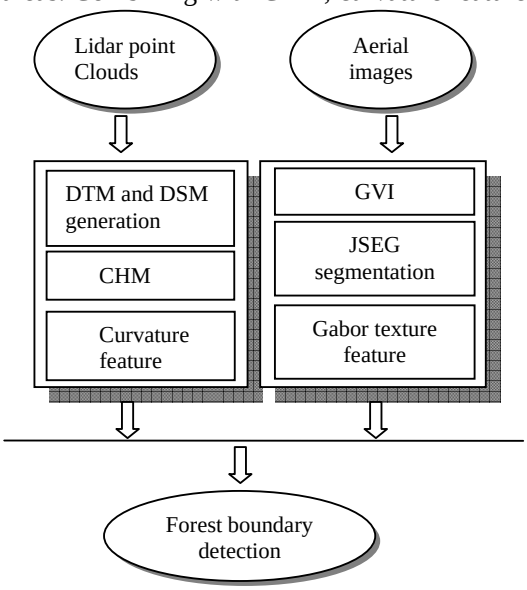

Fig. 1 Schematic workflow of overall process

2.2 Study Area

The aerial images in our database have been made available by Swiss Federal Office of Topography(swisstopo) with a scale of 1:30000, digitized, rectified, and mosaicked with 0.5-m resolution. We select the same places as in our finished project--monitorings bio diversity and landscape in the rural area to make a comparison with the manual interpretation of forest boundary. These places (as shown in Fig. 2) include different landscape types such as mixed industry areas, agriculture areas, wines areas and subalpine areas and each area is 1×1km.

Fig. 3 shows a 3D landscape simulation of one aerial image using height information from the surface with its landscape type belongs to Swiss midlands forest area.

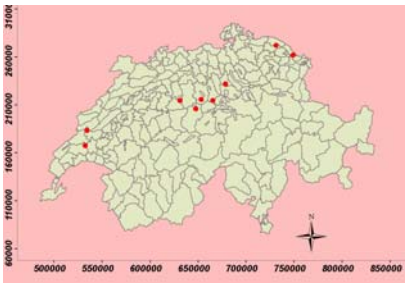

Fig. 2 Study areas

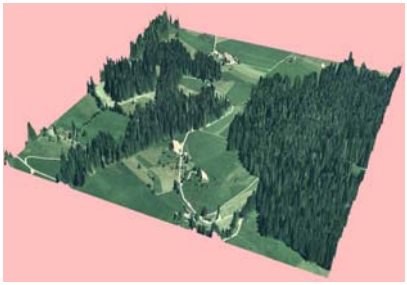

Fig.3 A 3D landscape simulation

2.3 The LIDAR data and Canopy Height Model

The LIDAR data was acquired between 2001 and 2004 by swisstopo. Average flight height above ground was between 100m and 150m. The footprint on ground varies between 0.8 m and 1.2 m. From the raw data, both a DTM and DSM are generated (as raw irregularly distributed points). The average density of the DSM data for whole Switzerland is 1-2 points / m^2. The CHM is obtained by calculating the difference between DSM and DTM. In Swiss NFI forest definition, the sample plot will probably be forest if the CHM value high than 3m, otherwise,

it will be defined as non-forest. The yellow part in Fig. 4b shows corresponding area where CHM>3m of the aerial images in Fig. 4a. From the images it can be seen that in some building areas CHM will larger than 3m. And with the given LIDAR data, CHM is not a uniform distribution. In some parts

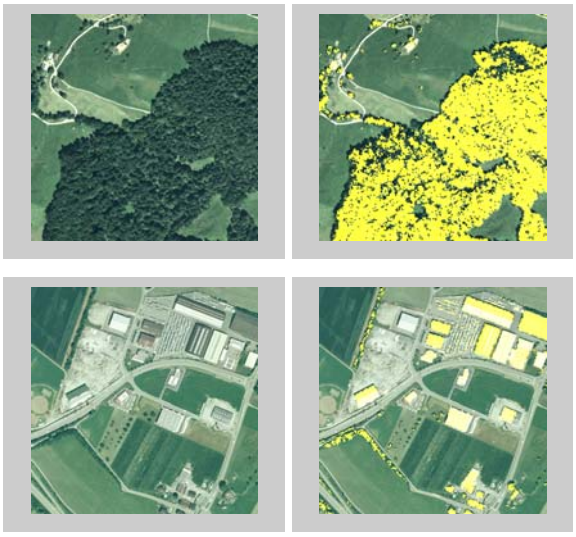

Fig. 4a Aerial images

Fig. 4.b Areas where CHM>3m

inside the forest, the CHM data can be missing. If it is only based on CHM, the whole forest area can hardly be detected correctly.

2.4 Curvature feature from LIDAR

Curvature is a metric to measure the shape of the elevation. It is the second derivative of the surface or the slope of the slope. A positive curvature indicates the surface is upwardly convex at that cell. A negative curvature indicates the surface is upwardly concave at that cell. A value of zero indicates the surface is flat. Based on the curvature's definition, curvature value of the pixels in forest area as well as the edges of buildings has higher absolute value than other flat areas. On the other hand, curvature value of building's surface has smaller absolute value which is quite helpful to distinguish buildings from forest areas. Fig. 5 shows the curvature features of images in Fig. 4a. In our forest detection algorithm, we define that the average of the absolute curvature value of an area which belongs to a forest should larger than a certain value ψ.

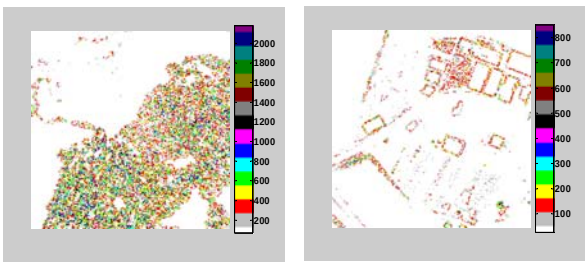

Fig. 5 Curvature features

2.5 Green Vegetation Index

Color is an important feature which we use to filter non-green vegetation areas in this paper. Simple image transformation may be useful in understanding image data. For instance, ratios might be helpful in enhancing difference between features in scenes. As we know, the Normalized Difference Vegetation Index (NDVI) is a measure of the amount and vigour of vegetation at the surface. NDVI is a non-linear transformation of the visible (red) and near-infrared bands of satellite information. Since the available true-color RGB aerial images don't allow calculating the widely used NDVI, we suggest an index which we name Green Vegetation Index (GVI) based on the use of green and red bands. For each aerial image, GVI is calculated as the ratio between green and red. Suppose R represent red, G represent green, then

$$GVI = G / R \quad (1)$$

Let $m = mean(GVI)$, then we define a threshold *th*,

$$th = \delta \times m \quad (2)$$

Depending on this threshold, we can filter non-green vegetation areas from the aerial images. Fig. 6 shows the result of the detected green vegetation area (which we name as GVI-forest) of images in Fig. 4a.

It can be seen that the detected green vegetation areas include forest, croplands, some agriculture used areas, etc. The results successfully remove most of the building areas which is helpful for forest detection.

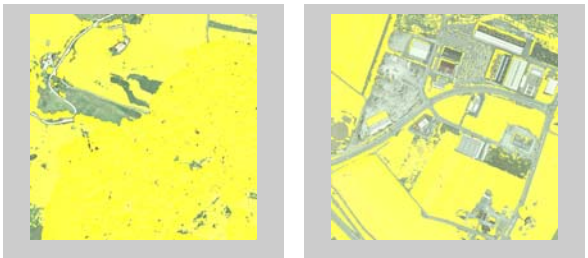

Fig. 6. GVI forest candidate areas

2.6 JSEG Segmentation

Segmentation is the process that subdivides an image into homogenous regions. JSEG[12] is one of the color image segmentation methods which provide robust segmentation results on a large variety of color images. First the image is quantized using an unsupervised color quantization algorithm [13] based on human vision perception. Following quantization, the reduced colors define color class labels while the color class number for each image is different. The image pixel colors are replaced by their corresponding color class labels which construct a class-map image. Let Z be the set of all image data points in the class-map, and $z=(x,y)$, m be the mean,

$$m=\frac{1}{N}\sum_{z\in Z} z \tag{3}$$

Suppose color has been quantized into C level, Z_i, $i=1,2.....C$. Let m_i be the mean of the N_i data points of class Z_i,

$$m_i=\frac{1}{N_i}\sum_{z\in Z_i} z \tag{4}$$

Let

$$S_T=\sum_{z\in Z}\|z-m\|^2 \tag{5}$$

and

$$S_W=\sum_{i=1}^{C} S_i=\sum_{i=1}^{C}\sum_{z\in Z_i}\|z-m_i\|^2 \tag{6}$$

S_T is the variance of points within the same class. S_W is the total variance of points belonging to the same class. Define,

$$J=S_B/S_W=(S_T-S_W)/S_W \tag{7}$$

It essentially measures the distance between different classes S_B between the members within each class S_W. A higher value of J implies that the class values are more separated from each other and members within each class are closer to each other and vice versa. The J-image is calculated over a moving window centered on the J - values. The size of the window is depending on the scale that is needed to segment an image. Normally, the basic window at the smallest scale is a 9×9 window without corners. A region growing and merging step based on the color similarity is used to segment based on the J-image. The color histogram for each region is extracted and the Euclidean distance in the color space is calculated and saved in a distance table. Each pair of regions with the minimum distance is merged together if the distance value reaches a threshold. One of the threshold parameters in JSEG controls the region merging within a range [0, 1.0]. Fig. 7 shows the segmentation results of Fig. 4a without region merging.

Depending on the combing height information obtained from CHM, curvature feature and GVI, forest areas which we name as CHM-GVI-JSEG forest can be obtained. Fig. 8 shows the detected CHM-GVI forest applying to the images in Fig. 4a.

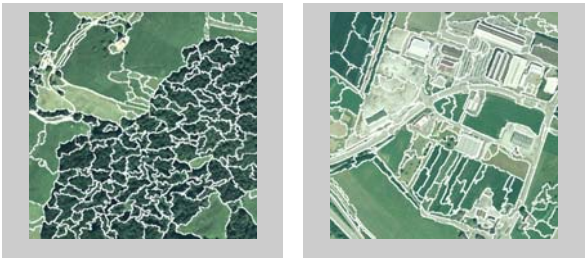

Fig.7 JSEG segmentation result

Fig.8 CHM-GVI-JSEG forest

2.7 Texture Features Extracted by Gabor Wavelet Transformation

Texture is another important feature which can be extracted from the images by different analysis algorithms. A large number of techniques have been proposed in the past two decades ranging from statistical approach to filtering approach. Gabor Filter [14, 15] belongs to one of the filtering approaches inspired by the multi-channel filtering mechanism discovered in neurophysiology which suggests that the visual system decomposes the retinal image into a set of sub-bands. A two dimensional Gabor function $g(x,y)$ and its Fourier transform $G(u,v)$ can be written as:

$$g(x,y)=\left(\frac{1}{2\pi\sigma_x\sigma_y}\right)\exp\left[-\frac{1}{2}\left(\frac{x^2}{{\sigma_x}^2}+\frac{y^2}{{\sigma_y}^2}\right)+2\pi jWx\right] \tag{8}$$

$$G(u,v)=\exp\left\{-\frac{1}{2}\left[\frac{(u-W)^2}{{\sigma_u}^2}+\frac{v^2}{{\sigma_v}^2}\right]\right\} \tag{9}$$

where $\sigma_u=1/2\pi\sigma_x$ and $\sigma_v=1/2\pi\sigma_y$. Let $g(x,y)$ be the mother Gabor wavelet, then this self-similar filter

dictionary can be obtained by appropriate dilations and rotations of $g(x,y)$ through the generating function:

$$g_{mn}(x,y)=a^{-m}G(x',y'),\ a>1,\ m,\ n = \text{integer}$$
$$x'=a^{-m}(x\cos\theta+y\sin\theta),\ \text{and}$$
$$y'=a^{-m}(-x\sin\theta+y\cos\theta) \quad (10)$$

where $\theta=n\pi/K$ and K is the total number of orientations. The scale factor a^{-m} in (10) is meant to ensure that the energy is independent of *m*. Such strategy as to ensure that the half-peak magnitude support of the filter responses in the frequency spectrum touch each other can be used to reduce the redundant information in the filtered images.[16] This result in the following equations to calculate the filter parameters σ_u and σ_v.

$$a=(U_h/U_l)^{\frac{1}{S-1}},\ \sigma_u=\frac{(a-1)U_h}{(a+1)\sqrt{2\ln 2}}$$
$$\sigma_v=\tan\left(\frac{\pi}{2K}\right)\left[U_h--2\ln\left(\frac{\sigma_u^{\,2}}{U_h}\right)\right]\left[2\ln 2-\frac{(2\ln 2)^2\sigma_u^{\,2}}{U_h^{\,2}}\right]^{-\frac{1}{2}} \quad (11)$$

where $W=a^mU_l$, U_h and U_l denote the lower and upper center frequency of interest. *K* is the number of orientation and *S* is the number of scales in the multi-resolution decomposition and $m=0,1,.....S-1$. In our experiments, $K=6$ and $S=4$

Using the Gabor filter set defined above, there are all 24 filtered images for an input aerial image. Since the local texture region of each sub-area after Jseg segmentation is homogeneous, the mean value μ_{mn} and the standard deviation σ_{mn} of the transform coefficients are used to present the sub-region. A feature vector constructed by μ_{mn} and σ_{mn} is represented as

$$f=[u_{00}\sigma_{00}\mu_{01}\sigma_{01}.....\mu_{35}\sigma_{35}] \quad (12)$$

2.8 Forest Boundary Delineation

Since regions that belong to the forest have been detected using CHM and GVI as CHM-GVI-JSEG forest, let,

$$f_{forest}=[u_{f00}\sigma_{f00}\mu_{f01}\sigma_{f01}.....\mu_{f35}\sigma_{f35}] \quad (13)$$

For each sub-area after JSEG segmentation with a feature vector,

$$f_{sub-area}=[u_{s00}\sigma_{s00}\mu_{s01}\sigma_{s01}.....\mu_{s35}\sigma_{s35}] \quad (14)$$

consider the distance between the two feature vectors defined as:

$$d(f_{forest},f_{sub-area})=\sum_m\sum_n d_{mn}(f_{forest},f_{sub-area}) \quad (15)$$

where
$$d_{mm}(f_{forest},f_{sub-area})=\left|\mu_{mn}^{\ forest}-\mu_{mn}^{\ sub-area}\right|+\left|\sigma_{mn}^{\ forest}-\sigma_{mn}^{\ sub-area}\right| \quad (16)$$

if the distance *d* smaller than a predefined threshold ξ, then the corresponding sub-area will belong to the forest, otherwise, it will belong to non-forest areas.

3 Experimental results and Conclusion

Fig. 9 represents some of the forest delineation results. Fig. 9a shows initial JSEG segmentation without region growing. Fig. 9b is the final forest boundary delineation (highlighted by white lines). Fig. 9c shows the manual interpretation of the forest boundary line (highlighted by red lines). The thresholds are empirically chosen as: $\psi=300$, $\delta=0.85$, $\lambda=0.4$ and $\xi=150$.

The experimental results indicate that combining with LIDAR data, after extending JSEG region merging with Gabor wavelet texture features, forest areas can be distinguished in a more semantic way. The introduction of GVI from aerial images and curvature feature are quite helpful for building's removing. Obviously, GVI finds most of the forest candidates while curvature feature gives chance to detect real forest area and constructs a feature vector

Fig. 9a JSEG segmentation

Fig. 9b final forest boundary detection

Fig. 9c manual forest

representing forest area using Gabor wavelet. Because of the unexpected point various density distributions, some of the forest area can be missing with the process CHM-GVI-JSEG forest. The additional Gabor wavelet texture features are suitable to make discrimination between forest and the other landscapes. By comparison with the manual forest boundary delineation results, the approach presented in this study offers an automatic process and delivers robust delineation of forest boundaries applied to aerial images with diverse illumination.

From the result, we can find that there are some places where the delineation results are different between our forest delineation result and manual interpretation. There are several reasons which can cause such kind of inconsistent. The first reason can be the gaps and shadow areas within forest. In our method, since there is no LIDAR data information and the texture feature is different from forest area for the gaps and shadows, the method will delineation gaps out of the forest while the interpreters delineated these areas as forests. The second reason can be the time delay between the taken time of aerial images and LIDAR data. The forest area may be cut or there can be some young forest areas regeneration which will make the inconsistence between the LIDAR data and aerial images. The third reason is the complete missing of LIDAR data. With the given point cloud of LIDAR data, in some forest area there can be not any point data within the sub area of JSEG segmentation which makes no chance for the forest detection.

Later on, further research is needed to find out whether or not other segmentation methods will be more suitable for homogeneous texture pattern detection which maybe helpful for more accurate forest area delineation. Currently, only typical midland areas have been investigated in detail, therefore how to extend the test area to alpine regions will be important for further verification of the proposed method.

References:

[1] H. Bachofen, F. Mahrer and e. al., Schweizerisches Landesforstinventar Ergebnisse der Erstaufnahme 1982-1986, Teufen: Kommissionsverlag Flück-Wirth, 1988.

[2] P. Brassel and Brändli, Schweizerisches Landesforstinventar Ergebnisse der Zweitaufnahme 1993-1995, Bern: Haupt, 1999.

[3] P. Brassel, Swiss national forest inventory: methods and models of the second assessment, Birmensdorf: Swiss Federal Research Institute WSL, 2001.

[4] M. A. Wulder and D. Seemann,Forest inventory height update through the intergration of lidar data with segmented Landsat, *Canadian Journal Remote Sensing*, vol. 29, 2003, pp. 536-543.

[5] E. Naesset,Determination of mean tree height of forest stands using airborne laser scanner data., *ISPRS Journal of Photogrammetry and Remote Sensing*, vol. 52, , 1997, pp. 49-56.

[6] F. Morsdorf, Meier, E., Kötz, B., Itten, K.I., Dobbertin, M. and Allgöwer, B.,LIDAR-based geometric reconstruction of boreal type forest stands at single tree level for forest and wildland fire management, *Remote Sensing of Environment*, vol. 92, 2004, pp. 353-362.

[7] C. J. e. a. J. Townshend,Global land cover classification by remote sensing - Present capabilities and future possibilities, *Remote Sensing of Environment*, vol. 35, 1991, pp. 253-255.

[8] W. B. C. M. A. Lefsky, and T. A. Spies,An evaluation of alternate remote sensing products for forest inventory, monitoring, and mapping in Douglas-fir forests of western Oregon *Canadian Journal of Forest research*, vol. 31, 2001, pp. 78-87.

[9] H. H. J. Hyyppä, et al,Accuracy comparison of various remote sensing data source in the retrieval of forest stand attributes, *Forest Ecology and Management*, vol. 128, 2000, pp. 109-120.

[10] A. Pekkarinen,A method for the segmentation of very high spatial resolution images of forested landscapes, *Int. J. Remote Sensing*, vol. 23, 2002, pp. 2817-2836.

[11] O. Hagner, Computer aided forest stand delineation and inventory based on satellite remote sensing, in *Proceeding from SNS/IUFRO workshop in Umeå 26-28 February 1990: The usability of remote sensing for forest inventory and planning*, Umeå: Swedish University of Agricultural Science, Remote Sensing Laboratory, 1990, pp. pp. 94-105.

[12] Y. Deng and B. S. Manjunath,Unsupervised segmentation of color-texture regions in images and video, *IEEE Transactions on Pattern Analysis and Machine Intelligence* vol. 23, 2001, pp. 800-810.

[13] Y. Deng, C. Kenney, M. S. Moore and B. S. Manjunath, Peer group filtering and perceptual color image quantization, in *Proc. of IEEE International Symposium on Circuits and Systems (ISCAS)*. vol. 4, 1999, pp. pp. 21-24.

[14] A.C.Bovik, M.Clark and W.S.Geisler, Multichannel texture analysis using localized spatial filters, *IEEE Transaction on Pattern Analysis and Machine Intelligence*, vol. 12, 1990, pp. 55-73.

[15] A.K.Jain and F.Farrokhnia,Unsupervised texture segmentation using gabor filters, *Pattern Recognition*, vol. 16, 1991, pp. 1167-1186.

[16] B.S.Manjunath and W. Y. Ma,Texture Feature for Browsing and Retrieval of Image Data, *IEEE Transaction on Pattern Analysis and Machine Intelligence*, vol. 18, 1996, pp. 837-842.